Power Optimization Modelling as a computational tool for Power Take Off design in wave energy converters.

AUTHORS:
Marcos Blanco*[A] marcos.blanco@ciemat.es
Isabel Villalba [B] isabel.villalba@ulpgc.es
Marcos Lafoz [A] marcos.lafoz@ciemat.es
Jorge Nájera [A] jorge.najera@ciemat.es
Gustavo Navarro [A] gustavo.navarro@ciemat.es
Miguel Santos-Herrán [C] msantos@carnegiece.com

***corresponding author**
AFFILIATIONS:
[A] CIEMAT (Centro de Investigaciones Energéticas, Medioambientales, y Tecnológicas). Avda. Complutense, no.40, CP28040, Madrid (Spain).
[B] UPLGC (Universidad de Las Palmas de Gran Canaria). Calle Juan de Quesada, 30, CP 35001 Las Palmas de Gran Canaria (Spain)
[C] Carnegie Technologies Spain S.L. Calle Claudio Coello, 24 – 4A2, CP. 28001 Madrid (Spain).

ABSTRACT.
This study describes a computational tool named Power Optimisation Modelling (POM), a methodology for optimizing the design parameters of the Power Take-Off (PTO) in wave energy converters (WECs). POM proposes a control optimization algorithm based on a differential evolution multi-objective approach, which seeks to maximize the electrical power extracted by the WECs while minimizing the associated design costs.
The methodology integrates a wave to wire (W2W) model in the time domain that includes a PTO loss model. It also considers the sea states where the WECs will operate, as well as constrains related to the rated force of the PTO. These distinctive features enable a comprehensive evaluation of the electrical energy generated by WECs and the obtaining of optimal PTO design parameters.
POM has been applied to a real case study involving the design of a linear generator-based PTO, operating under different sea states. The analysis combines four different WEC technologies and two sea states to assess the tool's effectiveness as a design methodology.
In conclusion, POM proves to be a versatile support tool for technology developers and researchers, enabling the optimization of PTO design to achieve an optimal balance between WECs manufacturing costs and generated power.
KEYWORDS. Wave to wire**/**Power Take-Off**/**Optimisation **/**Losses model/modular generator.

1 INTRODUCCIÓN.

In the search for solutions to mitigate climate change, marine renewable energies have emerged as a key element in the transition to a new energy model. Among marine renewable energies, wave energy is one of the most promising options. The vast resource available worldwide [1] [2], the technological advances in wave energy converters (WECs) over the last decade [3] [4]**,**and the successful implementation of numerous research and development (R&D) projects [5] have positioned wave energy a viable future option. However, WECs still face some challenges in achieving economic viability. Reports [6] [7] outline objectives for wave energy in Europe by 2030, proposing an installed and grid connected capacity of 496MW. The reports [6]

[7] [8] also suggest that optimized WEC solutions can reduce the Levelized Cost Energy (LCOE) to approximately 110 €/MWh without compromising efficiency.

Among the costs contributing to the LCOE, the manufacturing cost (CAPEX) plays a significant role. A key component of CAPEX is the manufacture of the energy extraction system or power take-off (PTO). Economic studies on WECs [9] [10] [11] identify CAPEX as a critical factor, emphasizing the optimization of WEC rated design characteristics as essential for reducing total costs.

Several previous studies have focused on methodologies to optimize PTO designs for WECs [12] [13] [14]**.** These optimization studies have firstly aimed to maximize WECs generated power by tuning the design parameters of PTOs. Other studies explore multi-objective optimization, balancing maximum power generation and cost reduction of the complete WEC [15] [16] [17] [18] [19] [20]**.**

The optimization method proposed in the Power take-off Optimization Modelling (POM) is based on a time domain Wave-to-Wire (W2W) model [21], providing a versatile numerical tool applicable to different WECs. Time domain hydrodynamic models have been studied for decades in works such as [22] [23], which analyse oscillating movements, accompanied with other foundational modelling studies [24] [25]. The POM presented in this paper expands and adapts the model to include the Power take-off (PTO) characteristics, as described in [26], including rated parameters, efficiency using a loss model, and operation constraints. In addition, the optimization algorithm considers these efficiency factors and constrains to maximize electric power rather than mechanical power [27].

Among PTO technologies, the ones based on linear electric generators [28] [29] offer significant advantages. This PTO topology minimizes potential system failures across conversion stages and improves control of the PTO extraction force [30] [31]**,** enhancing system efficiency.

POM also considers the sea states at the WECs installation sites, as the wave climate is a key design parameter to align PTO characteristics with the design problem based on the specific location [20]. In addition to maximize the electric power extraction, the POM introduces a new objective function: minimizing PTO manufacturing costs. This multi-objective algorithm enables POM to advance the state of the art in the optimization tools for the PTO design in WECs.

It is also important to point out that PTO efficiency should be integrated into control algorithms to maximize electrical power generation, rather than mechanical power [32] [33]. Optimizing mechanical energy leads the system to operate away from optimal electrical performance. The W2W model proposed in POM includes PTO system constrains, such as the force exertion limits [34] [35], which affect both the power generated and equipment cost. Consequently, the model can define the main the linear generator characteristics for a specific WEC [36]**.**

As an example, this paper applies POM to eight case studies -combination of four WEC technologies and two sea locations. This work is based on the SEATITAN project (Surging Energy Absorption Through Increasing Thrust And efficientNcy) [37] funded by the European H2020 Programme, GA No.764014. One of SEATITAN's objectives was the design of a versatile, modular and scalable PTO that could be integrated into four WECs technologies, since SEATITAN consortium included four WEC technology developers [38] [39] [40] [41]. The project involved the design of a novel azimuthal linear switched reluctance generator (AMSRM) [42], developed in a multi-translator configuration, adaptable to varying stroke and force requirements**.**

Once the PTO design objective was achieved, the focus shifted to identify solutions to maximize WEC electrical power output while minimizing manufacturing costs. With the aim of carrying out this objective, POM obtains the optimal AMSRM force and stroke values for the eight defined scenarios - combinations of four WEC technologies and two sea locations – while selecting the appropriate number of AMSRM modules for each case.

The paper is organized as follows: Section 2 summarizes the POM methodology, considering its fundamental parts: the time domain hydrodynamic model (W2W) (Section 2.1), the mathematical PTO loss model (Section 2.2) and the multi-objective optimization algorithm (Section 2.3). Sections 2.1 and 2.2 are described using a particular WEC case study - Wedge Global (WGwec) [41] - selected from the SEATITAN project. This WEC technology has been simplified for better understanding of the POM methodology. Section 3 describes the analysis and results of applying POM to four WEC technologies and two different locations, demonstrating the adaptability to different PTO configurations. Section 4 discusses the results obtained from POM evaluation as PTO design tool. Finally, Section 5 presents the main conclusions of the study.

2 POWER TAKE-OFF OPTIMISATION MODEL (POM).

The main phases of the POM are summarized in Figure 1. The POM consists of a W2W model in the time domain, which – in addition to the prime mover dynamic model - includes an integrated control strategy and a PTO loss model. The W2W model takes as input variables, or supra-parameters, the WEC and its location (sea states), where supra-parameters refer to parameters that cannot be modified during the optimization process. A nominal efficiency of 85% (in terms of electrical losses) is assumed, based on simulation analysis and laboratory testing of the specific linear electrical generator consider (AMSRM) [42].

Additionally, the POM incorporates a multi-objective optimization algorithm. The search space consists of two variables: the rated force and rated stroke of the PTO, which represent the representative characteristics of this PTO topology. The multi-objective optimization considers two objective functions: maximizing the electrical PTO power output and minimizing the PTO fabrication costs (CAPEX).

Both the PTO loss model and the W2W have been developed in a MATLAB© software environment, widely used in industrial developments for simulation purposes. Since only basic libraries were employed, there is a possibility to migrate the tool to open-access coding platforms such as OCTAVE, or to generate an open-access executable version of the POM for broader use.

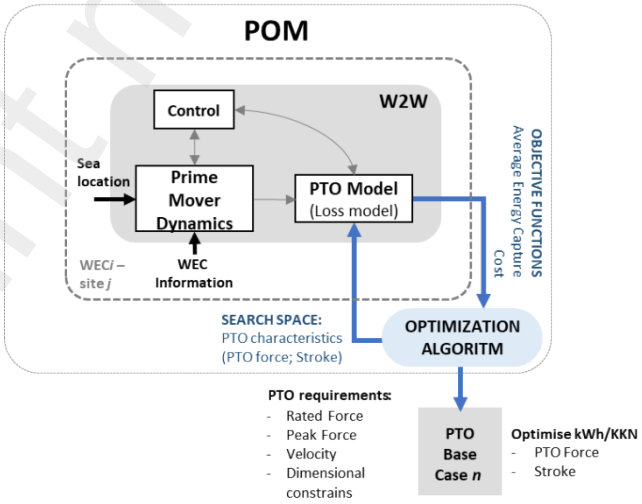

Figure 1. Diagram and scheme of the Problem Optimization Modelling (POM).

Subsections 2.1, 2.2, and 2.3 will explain in detail the POM subsystems and their main characteristics.

2.1 Description of the time-domain model of the prime mover.

The W2W model represents the whole energy conversion chain, from wave-device interaction to the resultant electrical energy, including models such as WEC model and PTO model. On a first step, the WEC model is based on linear wave theory and potential flow, and it is adapted from [21] [43]. In essence, it is the application of Newton's 2nd law, considering hydrodynamic and external forces.

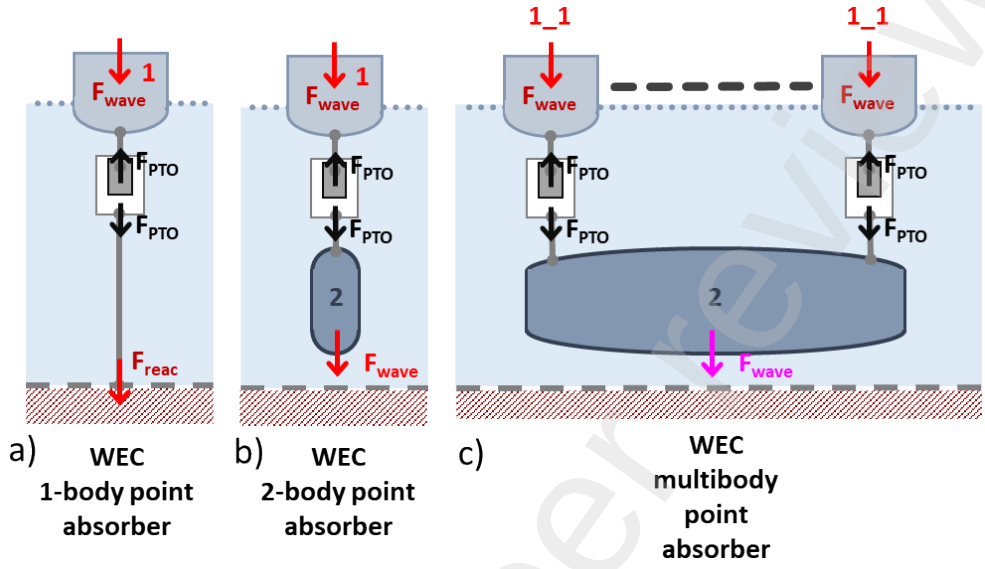

Figure 2. Topology type WEC. a) one-body point absorber. b) two-body point absorber. c) Multibody point absorber.

This study considers the two-body point absorber as the selected WEC topology. It consists of: the top floater and the spar-plate (see Figure 2.b). Its dynamic performance is based on the relative movement between these two bodies, with the study focusing on movement restriction to the z-axis (heave movement). The prime mover's heave movement is used by the PTO to extract energy from ocean waves.

The W2W model in the frequency domain for a two-body point absorber is defined in equations (1) and (2), where (1) corresponds to the floating body and (2) to the submerged body.

$$m_1 \cdot \frac{\delta^2 z_1}{\delta t^2} = \sum F = F_{mec_1} + F_{s1} + F_{r11} + F_{r12} + F_{mec_{12}} + F_{e,1} - F_{PTO} = -R_{mec_1} \cdot \frac{\delta z_1}{\delta t} - \cdot z_1 - R_{r11} * \frac{\delta z_1}{\delta t} - R_{12} * \frac{\delta Z_2}{\delta t} - m_{ad11} \frac{\delta^2 z_1}{\delta t^2} - m_{ad12} \cdot \frac{\delta^2 Z_1}{\delta t^2} - R_{mec_{12}} \cdot \left(\frac{\delta z_1}{\delta t} - \frac{\delta z_2}{\delta t} \right) + (F_{e,1} - F_{PTO}) \quad (1)$$

$$m_2 \cdot \frac{\delta^2 z_2}{\delta t^2} = \sum F = F_{mec_2} + F_{s2} + F_{r22} + F_{r12} + F_{mec_{12}} + F_{e,2} - F_{PTO} = -R_{mec_2} \cdot \frac{\delta z_2}{\delta t} - R_{r22} * \frac{\delta z_2}{\delta t} - R_{r12} * \frac{\delta z_1}{\delta t} - m_{ad22} \cdot \frac{\delta^2 z_2}{\delta t^2} - m_{ad12} \cdot \frac{\delta^2 z_1}{\delta t^2} - R_{mec_{12}} \cdot \left(\frac{\delta z_1}{\delta t} - \frac{\delta z}{\delta} \right) + (F_{e,2} - F_{PTO}) \quad (2)$$

Here, sub-index 1 corresponds to the floating body and sub-index 2 to the submerged body. The symbol * represents the convolution product and *j* represents the imaginary variable $\sqrt{-1}$. The forces and impedance represented are:

F_{ei} the excitation force to the "*i*" body,

R_{ri} the radiation resistance of the body due to body motion,
M_{adi} the added mass of the body i by the motion of the body,
R_{rij}, M_{asij} the mutual mechanical impedances,
R_{meci} the mechanical resistance,
M_i the total body mass,
S_i the coefficient of restoration or Archimedean force,
F_{PTO} the mechanical force developed by the electric generator.

The non-frequency dependent terms (M_i, S_i, R_{meci}, y F_{PTO}) are directly determined from the device dimensions. On the other hand, the frequency-dependent terms (F_{ei}, M_{adi},M_{adij}, R_{ri},R_{rij}) are hydrodynamic coefficients of the floating bodies and depend only on the geometry of the WEC. In this study, the hydrodynamic coefficients were obtained by using the WAMIT BIEM (boundary integral equation method) computational tool [44].
Equations (1) and (2) can also be represented using their equivalent electrical circuit (see Equations (3) and (4)). In this equivalent circuit, each mechanical variable has an equivalent electrical variable. forces are represented as voltages and velocities are equivalent to currents. Regarding impedances, mass corresponds to inductance, spring constants to the inverse of the capacitance and damping coefficients or mechanical resistances to electrical resistances (see Figure 3). Equations (3) and (4) has been reformulated in frequency domain according to [45] transforming variables in phasor form.

$$[R_{mec\_1} + R_{r11}] \cdot I_1 + [j \cdot (-1/(\omega \cdot C_1) + \omega \cdot (L_1 + L_{ad11}))] \cdot I_1 + (R_{r12} + j \cdot \omega \cdot L_{\infty 12}) \cdot = Z_{11} \cdot I_1 + Z_{12} \cdot I_2 = (U_{e,1} - U_{PTO}) \quad (3)$$

$$[R_{mec_2} + R_{r22}] \cdot I_2 + [j \cdot (-1/(\omega \cdot C_2) + \omega \cdot (L_2 + L_{ad22}))] \cdot I_2 + (R_{r12} + j \cdot \omega \cdot L_{\infty 12}) \cdot I = Z_{12} \cdot I_1 + Z_{22} \cdot I_2 = (U_{e,2} + U_{PTO}) \quad (4)$$

R_{mec_i} is the mechanical equivalent resistance of the body *i* (the sub-index "*i*" takes the value 1 for the floating body and 2 for the semi-submerged body),
R_{rij} is the radiation hydrodynamic resistance of the body *i* produced by the movement of the body *j*,
C_i is the capacity associated with the stiffness coefficient of the body *i;* L_i is the inductance associated with the mass of the body *I*,
L_{adij} is the added mass inductance of the body *i* produced by the movement of the body *j*,
U_{ei} is the excitation voltage of the body *i*; U_{PTO} is the voltage that represents the PTO force,
I_i is the current that that represents the velocity of the body *i;* Z_{11} is the body 1 total impedance,
Z_{22} is the body 2 total impedance; and Z_{12} and Z_{21} the mutual impedances [20].

Equations (3) and (4) can be expressed in matrix form (see (5)):

$$\begin{bmatrix} Z_{11} & Z_{12} \\ Z_{12} & Z_{22} \end{bmatrix} \cdot \begin{bmatrix} I_1 \\ I_2 \end{bmatrix} = \begin{bmatrix} U_{e,1} - U_{PTO} \\ U_{e,2} + U_{PTO} \end{bmatrix} \quad (5)$$

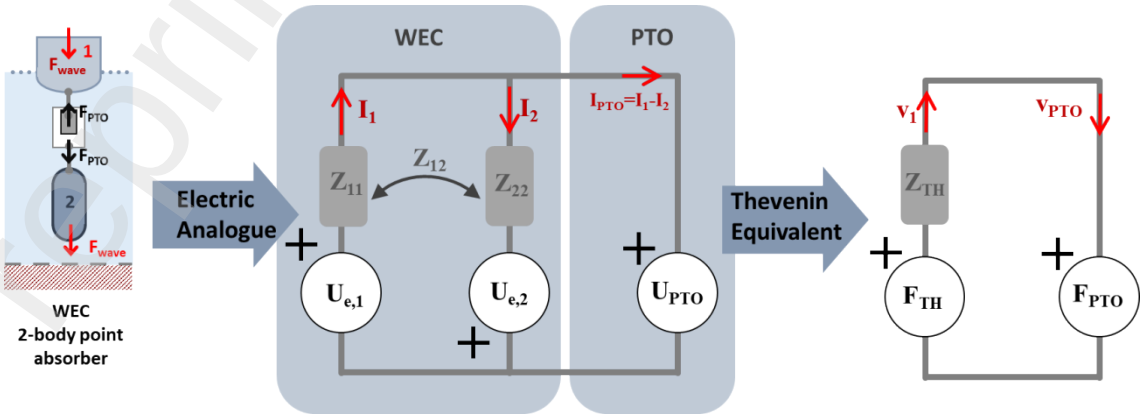

Figure 3. Electric Equivalent Circuits (a) 1-Body WEC; (b) 2-Body WEC [20].

The equivalent electric circuit of a two-body point absorber (Figure 3.b) can be simplified according to the Thevenin theorem [46] (see (6) and (7)) . From the PTO point of view, this simplified circuit is equivalent to the circuit diagram of a one-body point absorber from (Figure 3a) [20], where: U_{TH} is the Thevenin equivalent voltage (6) and Z_{TH} is the Thevenin equivalent impedance (7). These equations represent the simplified circuit.

$$Z_{TH} = \frac{(Z_{11} \cdot Z_{22} - Z_{12}^2)}{(Z_{11} + Z_{22} + 2 \cdot Z_{12})} = (Z_{11} \cdot Z_{22} - Z_{12}^2) \cdot (Z_{11}^* + Z_{22}^* + 2 \cdot Z_{12}^*)/ |(Z_{11} + Z_{22} + 2 \cdot Z_{12})|^2 \quad (6)$$

$$U_{TH} = ((Z_{11} + Z_{12}) \cdot U_{e,1} - (Z_{22} + Z_{12}) \cdot U_{e,2})/(Z_{11} + Z_{22} + 2 \cdot Z_{12}) \quad (7)$$

The mechanical power output - P_{mech} (8) - and the WEC electrical power output - P_{elec} (9) - are calculated from the previous equations. In this study, the power losses output - $P_{loss_{elec}}$ (10)- have also been considered, as detailed in the next subsection 2.2.

$$P_{mech}(t) = F_{PTO}(t) \cdot v_{rel}(t) \quad (8)$$

$$P_{elec}(t) = P_{mech}(t) - P_{loss_{elec}}(t) \quad (9)$$

Here, v_{rel} is the WEC relative velocity and $P_{loss_{elec}}$ is defined in (10).

$$P_{loss_{elec}}(t) = \frac{1}{R'_{PTO}} F_{PTO}^2(t) \quad (10)$$

Here, R'_{PTO} represents the losses in the PTO and is described in section 2.2.

2.2 Mathematical model of PTO losses and energy extraction control.

This section describes the PTO losses model and the energy extraction control subsystem. The PTO consists of an electrical linear generator and its power electronic converter. This type of PTO is especially suitable for heaving point absorber WECs, as its topology takes advantage of the linear movements and forces of the prime mover to generate electric energy without the need for any intermediate system [26]. The PTO loss model is used to calculate the WEC electrical output power, and it contributes to define the WEC control strategy. Both, the PTO loss model and the WEC control strategy will be integrated in the W2W model (see section 2.1). When integrating the PTO loss model into a mechanical W2W model, the development of a detailed electric PTO model may be discarded due to the faster dynamics of the electric variables. The switching frequency of the power electronic semiconductors is in the kHz range, much higher that the mechanical frequencies [47]. Therefore, a power loss model is used instead. For example, the developed PTO may establish its rated current at rated velocity within 10-20 ms, while the ocean wave periods are in the range of tens of seconds.

The PTO loss model is specifically parametrized for the azimuthal linear switched reluctance electrical generator (AMSRM) [42] designed as part of the SEATITAN Project [37]. However, this model can be also applied to other linear generator topology, such as induction generators or permanent magnet synchronous generators.

The following section describes the considerations for the PTO loss model and its relationship with the technological issues of the PTO. The magnetic losses, electric losses, power electronic losses and mechanical losses are considered in the PTO loss model [48]:

- **Magnetic losses:** Foucault and hysteresis [49]- dependant on the current oscillation frequency. These sources of losses are strongly dependent on the relative velocity between stator and translator [50]. Therefore, these losses could be neglected due the low displacement velocities of the generator.

- **Electric losses:** Joule losses [49] in connection cables and generator coils: dependant on electrical current. This source of losses accounts for about 95% of the total losses [47].This percentage is particularly significant in linear electric generators, where high forces and low velocities result in lower efficiency, especially when compared to conventional rotating generators.
- **Power Electronic losses:** Switching and conduction losses in the semiconductors - dependant on current amplitude and frequency. They are neglected due to the high efficiency of the power electronic system compared to other subsystems involved.
- **Mechanical losses:** Friction losses - dependant on the PTO velocity – were estimated to be around 1-2% based on previous tests with linear generator model [47] [51]. These losses can be neglected due to the low velocity.

Based on previous considerations, the conclusion is that the equation referring the total PTO power losses (11) can be simplified and only the term of electrical losses is considered (12).

$$P_{loss}(t) = P_{loss_{mag}}(t) + P_{loss_{elec}}(t) + P_{loss_{electronic}}(t) + P_{loss_{mech}}(t) \quad (11)$$

$$P_{loss}(t) = P_{loss_{elec}}(t) = P_{Cu}(t) \quad (12)$$

By incorporating Equations (8) and (12) into the development of (9), Equation (13) summarizes the expression for the $P_{elec}(t)$ in the PTO loss model.

$$P_{elec}(t) = P_{mech}(t) - P_{loss}(t) = F_{PTO}(t) \cdot v_{PTO}(t) - P_{Cu}(t) = F_{PTO}(t) \cdot v_{PTO}(t) - (t) = F_{PTO}(t) \cdot v_{PTO}(t) - R_{Cu} \cdot \left(\frac{F_{PTO_{rated}}}{I_{PTO_{rated}}}\right)^2 \cdot F_{PTO}^2(t) = F_{PTO}(t) \cdot (v_{PTO}(t) - R_{PTO}(t)) \quad (13)$$

Here: P_{elec} is the PTO generated electric power,
P_{loss} is the total PTO power losses,
P_{cu} is the Joule effect losses (winding losses),
F_{PTO} is the PTO force,
v_{PTO} is the relative velocity between the two parts of the linear generator PTO,
R_{cu} is the electric resistance of one phase of the PTO,
I_{PTO} is the electric current of one phase of the PTO. This term is developed in [42], where $F_{PTO_{rated}}$ is the PTO nominal force
$I_{PTO_{rated}}$ is the PTO current nominal value,
R'_{cu} is the coefficient to calculate the winding losses of PTO.

The complete PTO model could be formulated as an equivalent electrical circuit [52] [53], also representing the power losses (Figure 4).

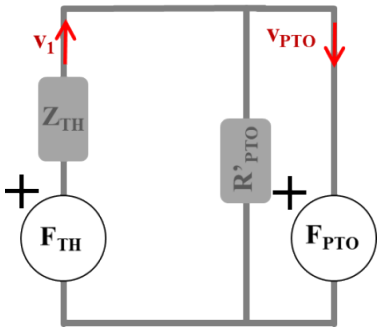

Figure 4. Electrical circuit of a WEC including a PTO losses model.

The electrical circuit represents a one-body WEC, however it is always possible to apply Thevenin's Theorem to formulate the dynamic behaviour for a two-body point absorber WEC (or even multi-body) as an analogue electrical dipole [34] [49] [53], viewed from the WEC's perspective. The analogue electrical circuit of one-body WEC is depicted in Figure 4, where the wave excitation force is represented by a voltage source, the mechanical hydrodynamic equivalent impedance by an electric impedance in series and the PTO force by another voltage source. Finally, the PTO losses are modelled as a resistance in parallel with the PTO voltage source (14).

$$R'_{PTO} = \frac{1}{R'_{cu}} = \left(\frac{F_{PTO_{rated}}}{I_{PTO_{rated}}}\right)^2 \tag{14}$$

Once the WEC dynamic performance has been represented by an equivalent electrical circuit, circuit analysis theory can be applied, using Boucherot's theorem, to determine the value of the force (F_{PTO}) leading to the maximum power extracted from the waves, taking PTO losses into account. These equations are used by the energy extraction control subsystem.

$$Z_{PTO_{OPT}} = \left(\frac{R'_{PTO} \cdot Z_{WEC}}{R'_{PTO} + Z_{WEC}}\right)^* \tag{15}$$

$$F_{PTO_{OPT}} = \frac{F_{TH}}{2} \cdot \frac{R'_{PTO} \cdot Z^*_{TH}}{R'_{PTO} \cdot R_{WEC} + |Z_{TH}|^2} \tag{16}$$

$$\upsilon_{PTO_{OPT}} = F_{TH} \cdot \frac{1 + 2 \cdot Z^*_{TH}}{2 \cdot R'_{PTO} \cdot R_{TH} + 2 \cdot |Z_{TH}|^2} \tag{17}$$

Here the symbol ■* stands for complex conjugate, and "|■|" stands for absolute value.
In the case of a two-body WEC, F_{TH} is the equivalent force resultant from the application of the Thevenin's Theorem simplification. Z_{TH} is the total mechanical impedance, and $Z_{PTO_{OPT}}$ (15), $F_{PTO_{OPT}}$ (16) and $\upsilon_{PTO_{OPT}}$ (17) the optimal values obtained under optimally controlled conditions. The above expressions can be formulated as a function of the PTO efficiency term -η- (18) and (19).

$$\eta = \frac{P_{elec}}{P_{mech}} = 1 - \frac{P_{loss}}{P_{mech}} = 1 - \frac{R'_{cu} \cdot F^2_{PTO}}{\upsilon_{PTO} \cdot F_{PTO}} = 1 - \frac{F_{PTO}}{R'_{PTO} \cdot \upsilon_{PTO}} \tag{18}$$

$$R'_{PTO}(\eta_{rated}) = \frac{1}{1 - \eta_{rated}} \cdot \frac{F_{PTO_{rated}}}{\upsilon_{PTO_{rated}}} \tag{19}$$

Here, η is the efficiency of the PTO in generator mode (18) and η_{rated} is the efficiency at rated force and velocity.
It is important to note that if R'_{PTO} (19) tends to an infinite value, the PTO has no losses, and the expressions coincide with those already developed in the Energy Maximizing Control (EMCs) theory, based on linear models [31]. Consequently, Equations (15), (16) and (17) can be translated into the following optimal control expressions in (20).

$$Z_{PTO_{OPT}} = Z^*_{TH};\ F_{PTO_{OPT}} = F_{TH} \cdot \frac{Z^*_{TH}}{R_{TH}};\ \upsilon_{PTO_{OPT}} = \frac{F_{TH}}{2 \cdot R_{TH}} \tag{20}$$

In addition, the $F_{PTO_{OPT}}$ should be limited to its rated value, due to its high impact in the energy extraction results [35] [54] [55].

2.3 Description muti-objective optimisation algorithm.

This section describes the multi-objective optimisation algorithm. A differential evolutionary algorithms (DE) [56] has been modified and adapted to solve multi-objective problems (MODE) [57].
The PTO main characteristics selection is posed as an optimization mathematical problem, and in this context, the objective functions and the variables of the search space has to be defined.

2.3.1 Objective functions

The goal is to optimise (to maximise, in this case) the average electrical power generated and to optimise (to minimise, in this case) the generator cost. In this context, the two objective functions considered in the optimization problem are:

- The maximization of the generated power by the complete system.
- The minimization of the cost of the PTO.

The average electrical power is evaluated using a W2W model (sub sections 2.1 and 2.2), by simulating every relevant sea state in each scenario, determined by the WEC type and location. The generator cost is assessed as a function as shown in (21) and according to [27].

$$cost = C_0 + C_1 \cdot S_{PTO_{rated}} + C_2 \cdot F_{PTO_{rated}} \tag{21}$$

Here, C_0 represents engineering costs, C_1 is related with the rated force and the number of scalable modular PTO units, C_2 is related with the length of the translator, $S_{PTO_{rated}}$ represents the PTO rated stroke, and $F_{PTO_{rated}}$ the rated force.

Figure 5a shows a scheme of the AMSRM module and its main parts: translator and stator. This type of electric machine can be designed based on stacking a certain number of modules (or stators), where the total force is the result of multiplying the number of modules by the nominal force of one module. The stroke of the electric machine is related to the number of stator modules and the total length of the translator, including the nominal stroke. For this reason, in a particular PTO solution, stroke and force can be selected independently, and similarly, in the cost function, stroke and force appear to be independent terms.
Figure 5b shows a plot with the relationship between PTO costs and PTO force for different PTO designs. In this case, the cost evaluation is simplified, based on manufacturing data of SEATITAN project used in [55], and normalized using the maximum budget as a base cost value. The direct relation between PTO force and PTO cost highlights the need for design strategies, such as optimizing the PTO design using a modular system, minimizing the dimensions of mechanical systems or using materials that reduce the weight.
This paper proposes a modular PTO design (see section 4). The result of this approach is a versatile PTO which can be adapted to any type of WEC.

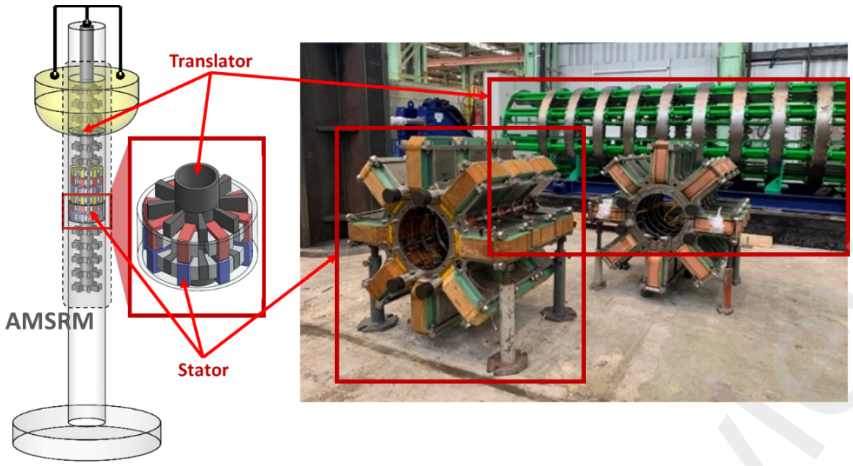

Figure 5. AMSRM module scheme developed in SEATITAN project.

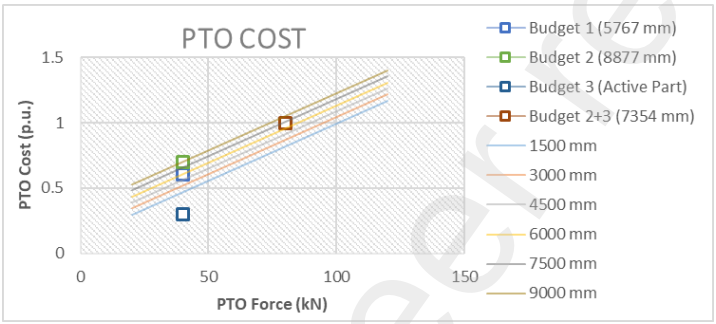

Figure 6. Plot about the relation between PTO costs and PTO force for different PTO designs in SEATITAN project.

Due to the fact that the POM is used to determine the most appropriate PTO, the variables to be selected are the basic characteristics of this PTO topology: the rated force and the rated stroke, constituting the search space of the optimization algorithm.

The MODE algorithm operates as described in Figure 7. The Target location and WEC type are predefined as supra-parameters (parameters that remains fixed during the optimization). Thus, one optimization or one execution of the POM has been carried out in each scenario, defined by WEC and target location. The "individuals" (solutions) are defined as PTO configuration, with specific values of each of the search space variables, force and stroke. For instance, individual no. 1 could represent a PTO with 50 kN of force and 6 m of stroke). In the first "generation" (iteration), a random "population" (set) of individuals is defined, called $\mathbf{P_0}$**.** The W2W model, parametrised for a given WEC and using the information of every individual, is evaluated for every sea state of the chosen location. The results of the two objective functions for $\mathbf{P_0}$, obtained for each sea state, are: electrical power generated (weighted with the relative occurrence of each sea state) and PTO cost.

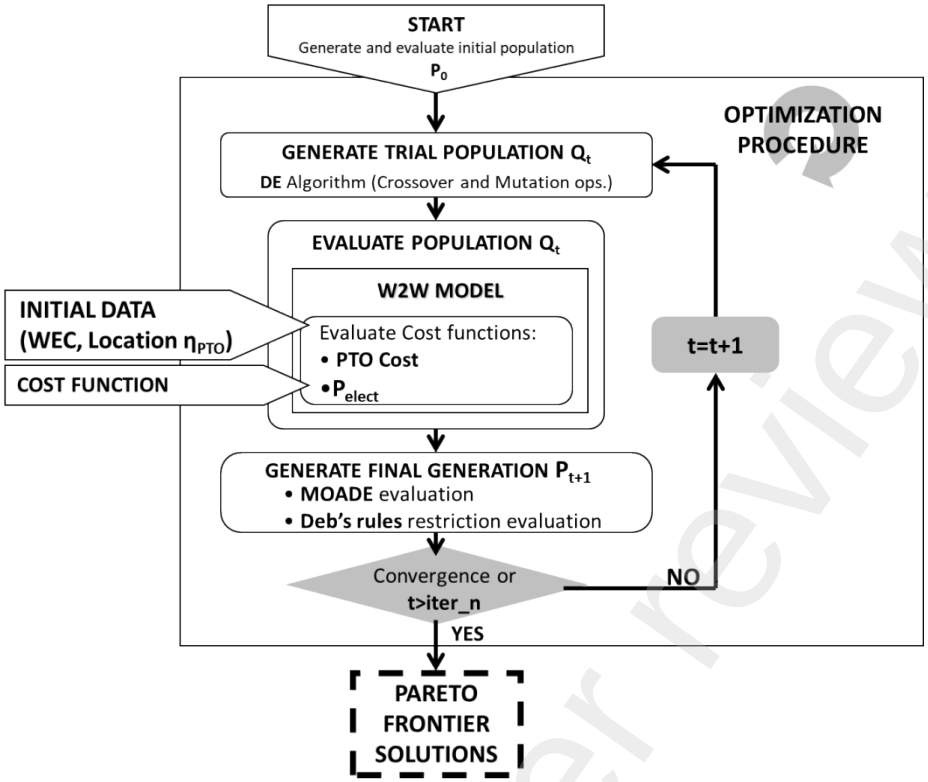

Figure 7. Scheme of the optimization algorithm application.

At this point, - considering an iteration or generation **t=1 -** once the objective functions of each individual of a population $\mathbf{P_t}$ have been evaluated, the optimisation algorithm proceeds with the generation of a trial population $\mathbf{Q_t}$. The values of the search space variables of each individual of the trial population $\mathbf{Q_t}$ are generated using the DE strategy (Mutation and crossover methods [17] [56]) based on the values of the initial population $\mathbf{P_t}$ (see Figure 8Figure 8). Every individual in the trial population $\mathbf{Q_t}$ is evaluated.

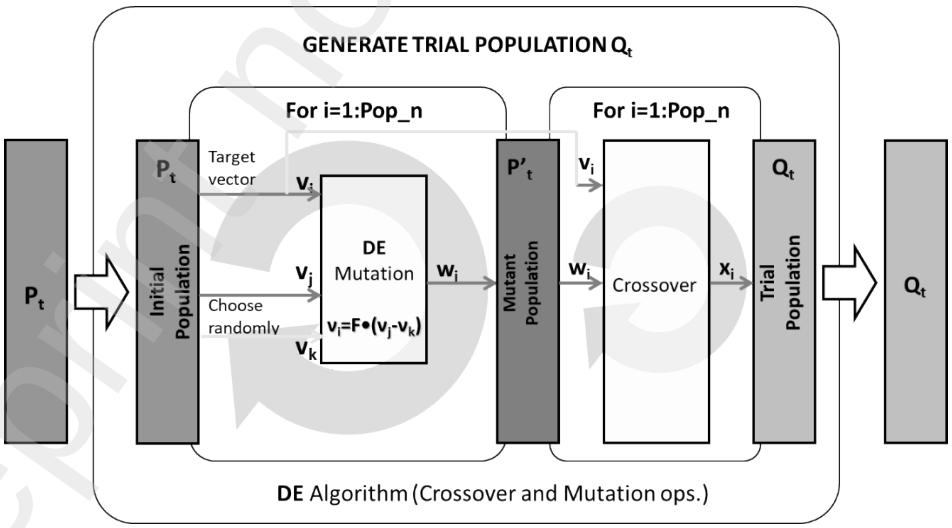

Figure 8. Scheme of the Differential Evolutionary Algorithm to generate trial population Qt.

The best solution in the population sets $\mathbf{Q_t}$ and $\mathbf{P_t}$ are selected by means of the method that uses the algorithm NGSA-II [58], based on the non-dominated sorting and the Crowding distance methods (see Figure 9).

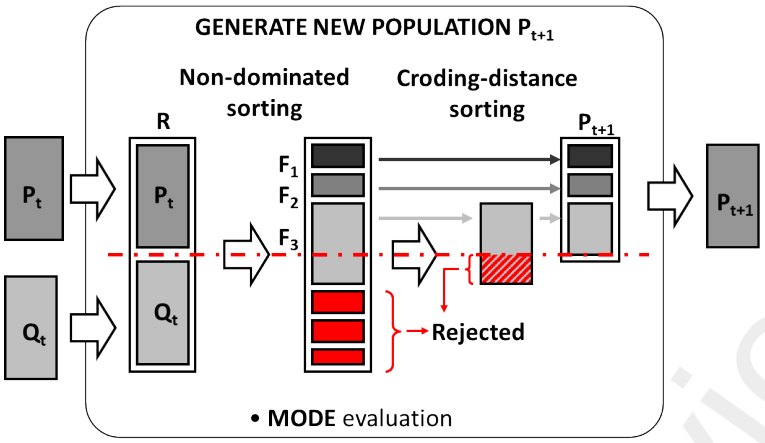

Figure 9. Pareto Selection of the best options of [Qt,Pt] and to generate Pt+1.

Since the optimisation problem is multi-objective, there is not a unique optimal solution, but a set of optimal solutions known as "Pareto front". Solutions on the Pareto front are optimal because there is no other better solution in both objective functions. All these solutions satisfy the conditions of maximizing the electrical power production and minimizing the PTO cost.

3 PTO DESIGN RESULTS OBTAINED VIA POM.

This section summarizes the results of the PTO design obtained using POM. Eight scenarios (combination of WEC type and location) have been considered, taking into account two different locations for each of the four WEC types evaluated (see Table 1): a semi-submerged single body point absorber (i.e. inspired by its working principle) similar to CORPOWER technology [38] (CPwec - Figure 2.a); a single body point absorber with structure fixed to the sea bed, similar to SEACAP technology [39] (SCwec - Figure 2.a); a multibody set of point absorbers with a common structure, similar to CENTIPOD technology [40] (CNwec - Figure 2.c); and a two-body point absorber with a buoy and a plate, similar to WEDGE technology [41] (WGwec - Figure 2.b). The locations considered correspond to the test facilities: Aguaçadoura (Portugal [59], Bilia Croo Bilia Croo (UK - EMEC [60], Orkney (UK – EMEC [61], Semrev (France – Nantes [62], BIMEP (Spain – Vasque Country [63], and PLOCAN (Spain – Canary Islands) [64]. These eight scenarios are summarised in Table 1.

Table 1. Scenarios to be analyzed with the POM.

Nº. scenario	WEC technology	Location
1	CP – CorPower (CorPower WEC)	1 – Aguaçadoura
2	CP – CorPower (CorPower WEC)	2 – BiliaCroo
3	SC – SeaCap (HydroCap WEC)	1 – Orkney
4	SC – SeaCap (HydroCap WEC)	2 – Semrev
5	CN – Centipod (Centipod WEC)	1 – BiliaCroo
6	CN – Centipod (Centipod WEC)	2 – BiMEP
7	WG – W1 (WedgeGlobal WEC)	1 – Plocan
8	WG – W1 (WedgeGlobal WEC)	2– BiMEP

For a better understanding of the POM, the results for the specific scenario 7 (Table 1) are presented first. This scenario corresponds to the two-body point absorber WGwec [41] at PLOCAN [65] location, a test site in the Canary Islands (Spain). Using this case as an example, a selection methodology for the optimum solution is explained (see section 3.1). The optimal

solution is defined as the ideal values for the PTO parameters: stroke and power. This solution satisfies the optimization objective functions: max P_{elec} (13) and min $cost$ (21).

3.1 Exemplification of POM execution: results for one base case.

In a first stage, the methodology is applied simulating 9 representative sea states of the target location of the WEC device to evaluate the power extraction profile. In scenario 7, the location is PLOCAN (Figure 10 and Figure 11 show the sea location and the corresponding scatter diagram respectively). The sea states of the location are selected using a MAXDISS algorithm, as described in [66]. This approach reduces the number of sea states evaluated and simplifies the graphical representation of the results. A wave elevation time profile is generated considering the H_s (significant height) and T_p (peak period) of the sea state and a JONSWAP spectrum [67]. As a preliminary analysis of the WEC operating under the optimum control proposed in section 2.1, the W2W tool is used with regular waves in order to obtain the WEC power output profiles (mechanical and electrical) for different input wave periods, as shown in Figure 12. The power profiles for two cases are presented: (blue lines stand for mechanical power and brown lines stand for electrical power): (1) the lines marked with squares represents the case where the control does not account for the PTO losses; (2) the lines marked with circles correspond to the case where the PTO energy extraction control has been modified to take into account PTO losses. The PTO efficiency considered is 75%. This figure shows that in case (1), more mechanical power is extracted, but the excessive reactive mechanical power reduces the electric power generated. In some frequencies, the electric power even reaches negative values, which means that the system requires electric power from the grid to compensate the power losses.

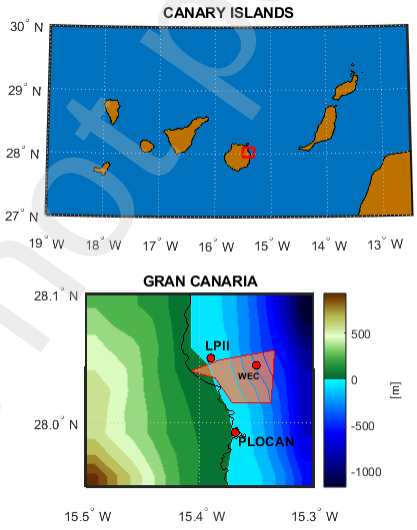

Figure 10. PLOCAN location and scatter diagram.

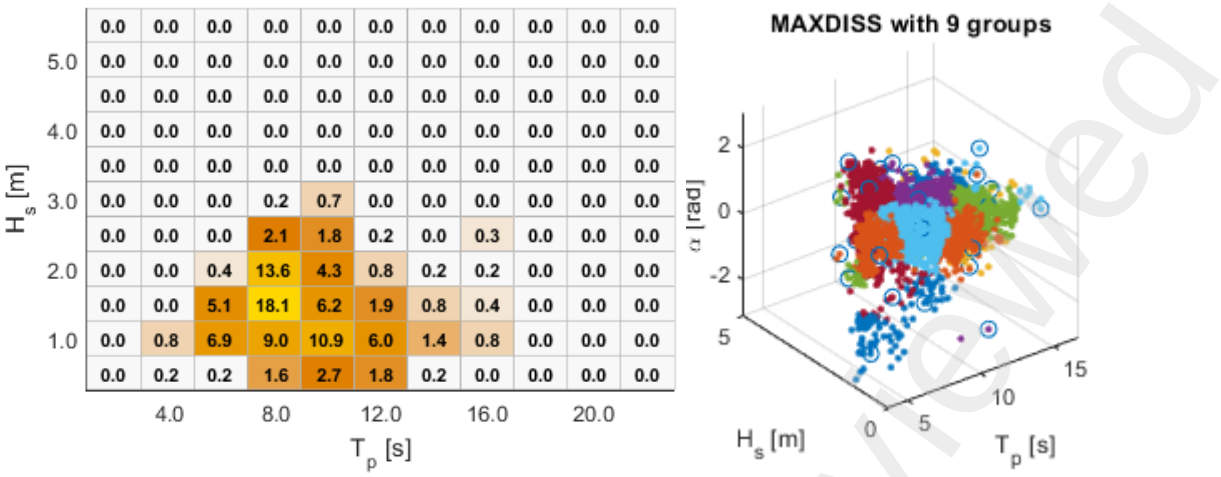

Figure 11. Scatter diagram and the nine sea states selected by MAXDISS for the PTO characterization methodology.

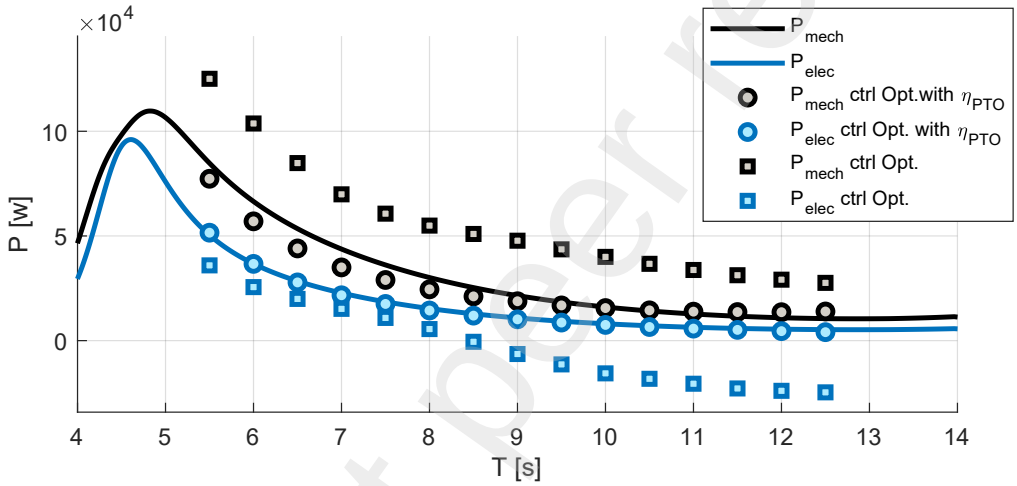

Figure 12. Electrical and mechanical power profiles for different input wave periods, and with two energy extraction controls.

In a second stage, the multi-objective optimization algorithm phase of the POM is executed considering the $F_{PTO_{rated}}$ and S_{PTO} as the search space variables, with the objective functions max (P_{ele}) and min ($cost_{PTO}$). However, due to preliminary information such as the PTO cost and efficiency, the ratio of generated power to cost is used in this case, which is inversely proportional to a PTO CAPEX/kW figure. The best selection criterion is the ratio of "generated electrical power" to "PTO cost". Nevertheless, this criterion can be adjusted according to the technology developers' needs by adding technical constrains, such as setting a maximum rated stroke or choosing the best solution from the Pareto front in terms of the Levelized Cost of Electricity (LCOE).

The graphical results of the execution of the POM for scenario 7 are shown in Figure 13. Figure 13a presents the PTO solutions evaluated during the MODE optimization in the search space defined by the variables $F_{PTO_{rated}}$ (N) and S_{PTO} (m). This search space is delimited by the lower and upper limit values for each variable (as indicated on the axes). Additionally, each PTO solution represented in the search space is presented with a colour depends on its value in each objective function (see Figure 13b and Figure 13c). The magenta curve plotted in the search space represent the zone of PTO solutions that belongs to the pareto frontier. Figure 13d represents the set of realizable solutions in the space of the objective functions ($P_{elecavg}$(W) and costs (p.u)) by representing the Pareto Front. A well-defined Pareto front can be observed.

The optimal PTO solution point is highlighted in both the search space (Figure 13a) and the objective function space (Figure 13d). In Figure 13d, the relationship between $P_{elecavg}$ (W) and costs (p.u) is also represented by the red dashed line, where the selected PTO solution (selected in form the Pareto Fortier solutions) is the PTO configuration with best $P_{elecavg}/cost$ ratio. The optimal solution is found at 109.26 kN of rated force and 2.664 m of maximum stroke.

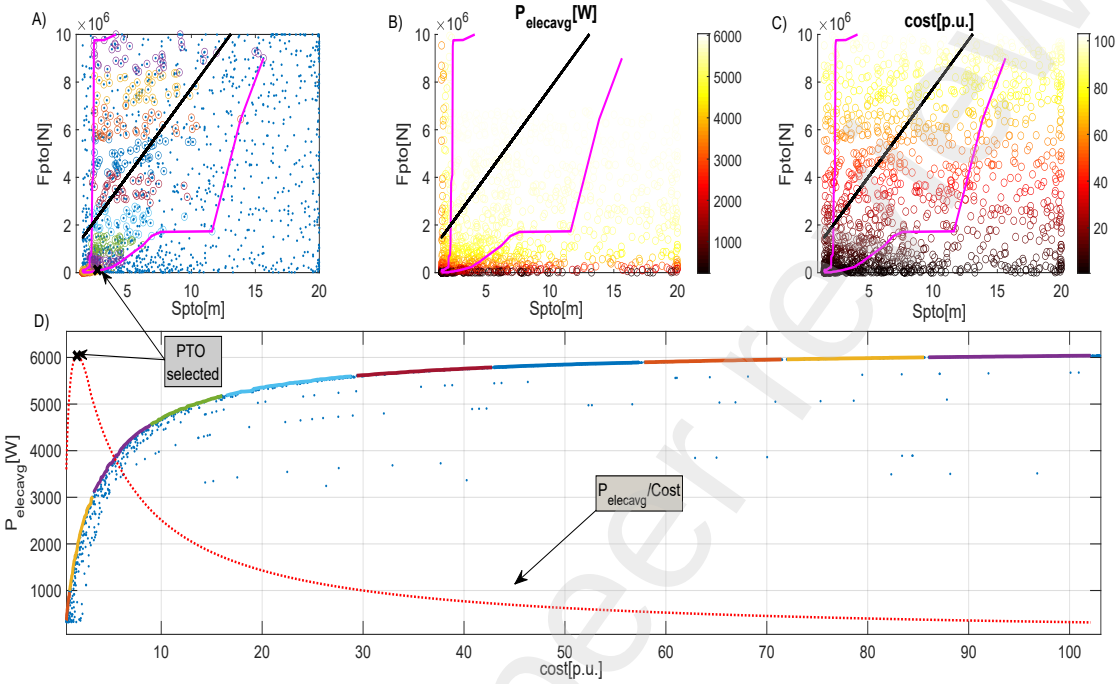

Figure 13. Pareto Frontier of scenario 7: a) b) c) respect to the search space variables; d) respect to the optimization functions.

3.2 Results of the POM execution for all considered cases.

The criterion for selecting the optimal solution after the execution of the POM has been chosen considering the differences in the LCOE that different WEC technologies may exhibit. LCOE costs may change depending on the PTO characteristics of each technology, such as weight or dimensions. The Pareto fronts have been obtained for the eight scenarios studied (see Figure 1-Annex). For all eight scenarios analysed, the optimal solutions continue to belong to the Pareto front obtained after the execution of the POM. As shown in Figure. 1 (Annex), although the configuration of the PTO can change in each case, it will still belong to the Pareto front of solutions identified after executing the POM. Table 2 summarizes the force and stroke values for the selected PTOs for each scenario, which corresponds to the PTO solution with the highest power-to-cost ratio.

Table 2. PTO configurations selected in each scenario.

Nº. scenario	WEC	Location	$F_{PTO_{rated}}$ [kN]	S_{PTO} [m]
1	CP	1	298.41	4.335
2	CP	2	260.97	3.205
3	SC	1	383.24	2.437
4	SC	2	236.36	2.332
5	CN	1	291.92	1.874
6	CN	2	269.10	2.961
7	WG	1	109.26	2.664
8	WG	2	144.66	2.273

The Figure 14 shows the PTO solutions evaluated in each of the eight scenarios, representing in each scenario: the Pareto frontier; the line $P_{elecavg}/cost$ ratio; and the optima PTO solution (selected as the best $P_{elecavg}/cost$ ratio solution). The Table 2 results are based in the plots of this Figure 14.

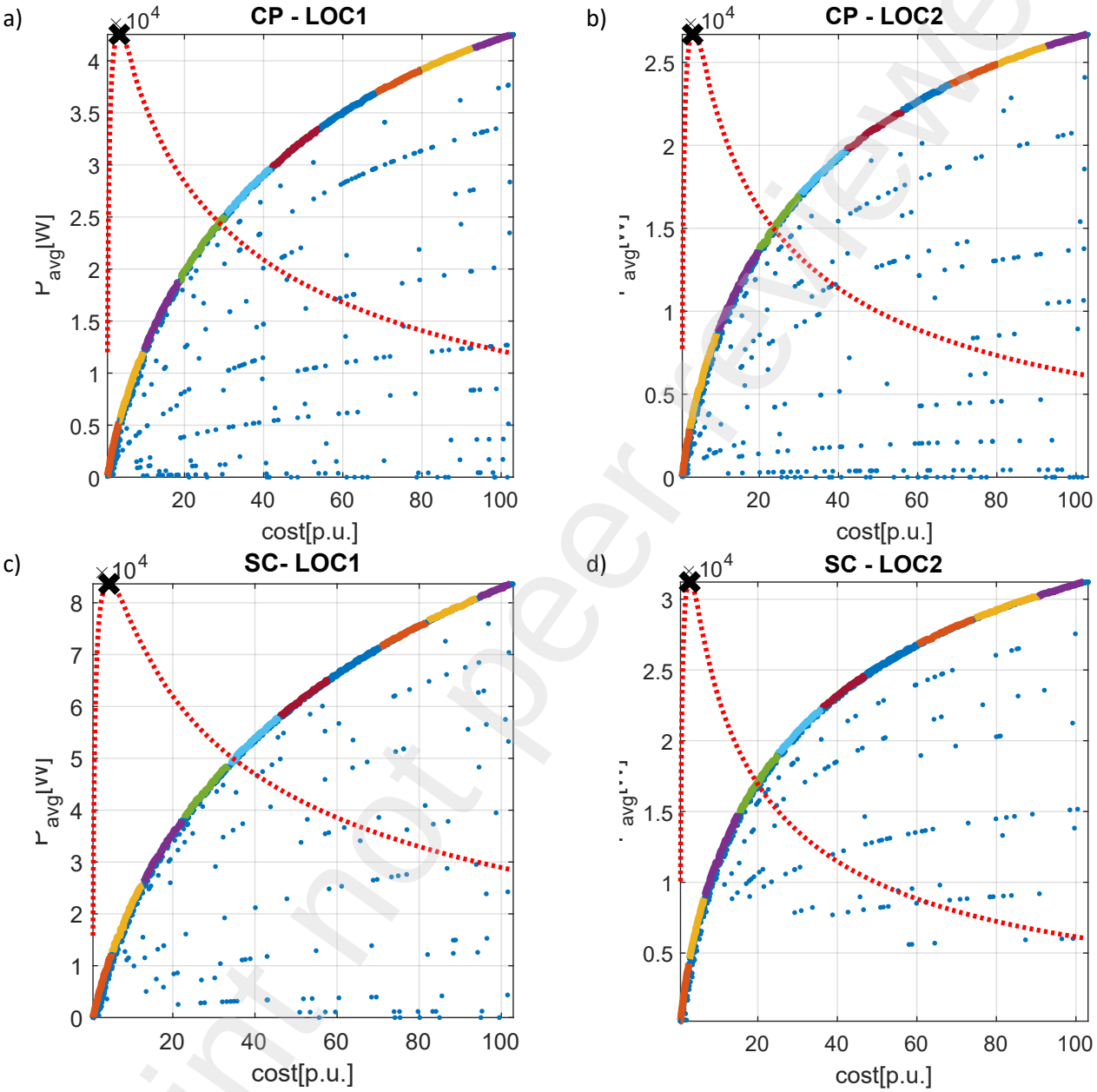

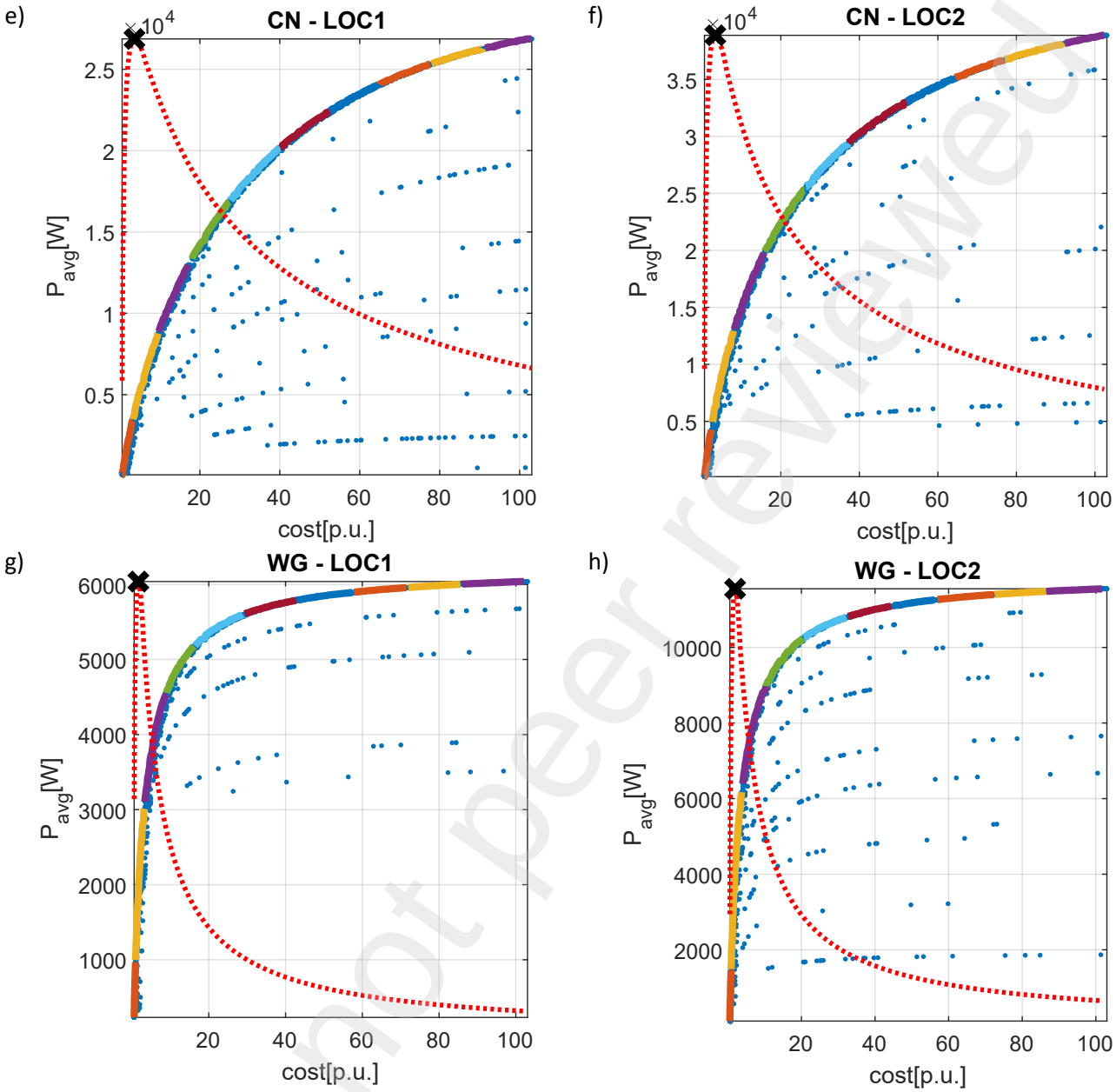

Figure 14. Pareto frontier of the eight scenarios.

4 APPLICATION OF POM RESULTS: SELECTION OF THE AMSRM MODULE TO BUILD THE FULL PTO.

Section 2.3 presented the relationship between the number of generator modules and the final P_{elec} (W) of the PTO, as well as its influence on the PTO *costs* (see Figure 5). Section 3 demonstrated the influence of the decision variables ($F_{PTO_{rated}}$ (kN) and S_{PTO} (m)) in obtaining the optimal PTO solution that satisfies the POM objective functions to achieve *max* P_{elec} and *min costs*. Consequently, the optimal number of generator modules was obtained using the POM.

Section 4 presents a case study applying the results obtained from executing of the POM for the 8 scenarios. The results in Table 2 were used to design an optimal PTO solution that addresses all 8 scenarios. This design was evaluated based on the characteristics of the AMSRM modules.

For this study, a range of AMSRM modules was evaluated, offering rated forces between 10 and 400 kN. The variables considered in designing the complete PTO are:

- Number of modules: This was minimised to simplify the PTO. Moreover, since the total generator length depends on the stroke and the number of modules, reducing the number of modules helps to fit the PTO within the available space in the WEC.
- Excess in resulting force: The overdimensioning of the PTO caused by the integer nature of the number of modules count was also minimised.

Figure 15 presents the results for various PTO configurations across the 8 scenarios. The average number of modules (blue line) and the nominal force for each module (kN) are shown, along with the average force excess percentage (%) relative to the optimal force calculated by the POM (orange line). Using the double criteria of minimizing both the number of modules and force oversizing, Figure 15 highlights a compromise solution consisting of a 40- kN module. This configuration minimizes the PTO force excess for the 8 scenarios while maintaining a relatively low average number of modules (see red point). The complete numerical results are included in Table 1-Annex.

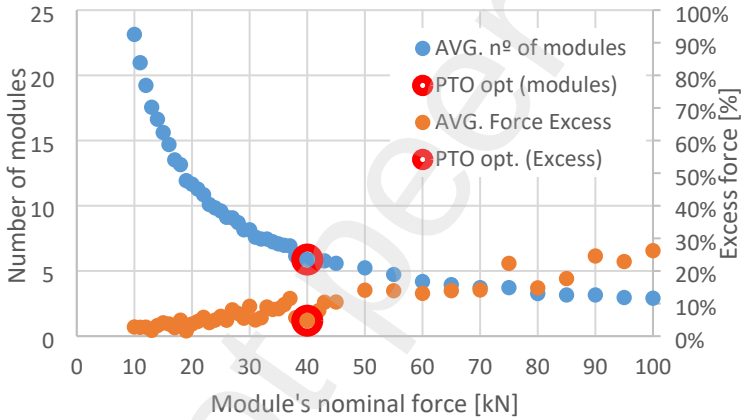

Figure 15. Average number (of 8 scenarios) of PTO modules, and Force excess for different configurations of PTO (different values of rated force of PTO module).

A nominal efficiency of 85% was assumed in all the cases presented in the figure. This value was derived from the preliminary electromagnetic model of the linear generator considered (AMSRM) [42].

In a final step, the influence of PTO efficiency on the results was evaluated. Based on the methodology, the rated force value of the AMSRM module was determined to be 40 kN. However, the actual efficiency may differ from the design phase value when applied to a real AMSRM prototype. This variation could result from factors such as modification to the magnetic circuit due to mechanical implementation requirements or increased conduction resistance caused by electrical connections.

The module selection analysis was repeated for alternative efficiency values to assess the impact the impact of this variable on the results. Table 3 presents the results of the parametric analysis OFAT (one factor at time sensitivity analysis) of the AMSRM module force. The base efficiency value was established at 85%.

Table 3. Percentage of PTO characteristics variation and of the objective functions with respect to a variation in the AMSRM efficiency (OFAT [one factor at a time] sensitivity analysis).

SCENARIO	OFAT nu (F_pto analysis)

WEC	no._location	F_{pto} (η: 75%)	F_{pto} (η: 80%)	F_{pto} (η: 85%)	no. pto modules (η: 75%)	no. pto modules (η: 80%)	no. pto modules (η: 85%)	Δno (nu:75%)	Δno (nu:80%)
CN	1	361,0	325,0	**291,9**	10	9	**8**	2	1
CP	1	327,9	300,5	**298,4**	9	8	**8**	1	0
SC	1	418,2	413,6	**383,2**	11	11	**10**	1	1
WG	1	140,0	128,9	**109,3**	4	4	**3**	1	1
CN	2	306,7	290,5	**269,1**	8	8	**7**	1	1
CP	2	264,5	278,0	**261,0**	7	7	**7**	0	0
SC	2	291,1	274,0	236,4	8	7	6	2	1
WG	2	163,8	148,3	144,7	5	4	4	1	0

The variables F_{PTO} and number of AMSRM modules were selected to analyse the impact of the different efficiency values. These variables, resulting of the POM, constrain and define characteristics of the AMSRM generator. Their variations relative to the selected base efficiency were analysed.

The results in the table show that the required nominal PTO force tends to increase as efficiency decreases. However, this results in a marginal increase of 1-2 AMSRM modules to achieve the required force in each scenario. In the case of CP technology at location 2 (BiliaCroo), it is not even necessary to vary the number of modules.

5 CONCLUSIONS.

From the perspective of computational tools, the analysis presented in this paper concludes that the POM is a valuable design tool for optimizing WEC design. The proposed POM establishes a universal methodology that can be adapted and applied to any type of WEC technology and location. This statement is supported by the results obtained from applying the POM to 8 different scenarios, which include 4 distinct technologies and 2 sea locations. Consistent and positive results were obtained, as clearly illustrated in the Pareto front solution graphs and the optimal PTO selection graphs.

Additionally, it is concluded that the POM is a highly applicable design tool. By applying the POM results to the modular design of the particular linear generator topology AMSRM as part of the PTO design optimization, a balanced solution is obtained for all 8 scenarios. This solution exhibits common design characteristics, such as a PTO force per module (F_{PTO} per module) of 40kN and a specific number of modules. These results demonstrate that the solution provides a versatile design that maximize electrical output power, P_{elec} (max) while minimizing the PTO costs (LCOE). Specifically, the application of the POM reveals information about a design parameter that influences the length of the PTO, the stroke (S_{PTO}). The analysis of S_{PTO} underscores the importance of this parameter, as it influences not only the minimization of CAPEX but also the determination of the optimal modular system design.

Finally, the sensitivity analysis of PTO efficiency shows that the selection of the maximum force and stroke is relatively not affected by potential variations in the efficiency figure.

In conclusion, the study demonstrates that optimization algorithms, when integrated into an appropriate methodology and computational environment, are powerful mathematical tools that contribute significantly to WEC design. This has been clearly demonstrated with the POM proposed in this study.

Acknowledgements

The authors would like to thank WavEC Renewables Offshore and, in particular, the researcher Mr. Miguel Vicente, for all the support provided in the hydrodynamic modelling of the wave energy converters integrated into the final code, as well as the WEC developers participating as partners in SEATITAN.

Funding: This research, developed under the Project SETITAN (ID: 764014), has received funding from European Union's Horizon 2020 research and innovation programme under H2020-EU.3.3.2. - Low-cost, lowcarbon energy supply (LCE-07-2016-2017).

6 References

[1] G. Mork, S. Barstow, A. Kabuth and M. T. Pontes, "Assessing the global wave energy potential," in *29th International Conference on Ocean, Offshore and Arctic Engineering (OMAE)*, ASME, 2010.

[2] K. Gunn and C. Stock-Williams, "Quantifying the global wave power resource," *Renewable Energy,* vol. 44, pp. 296-304, 2012.

[3] A. F. O. Falcão, "Wave energy utilization: A review of the technologies," *Renewable and Sustainable Energy Reviews,* vol. 14, no. 3, pp. 899-918, 2010.

[4] A. Pecher and J. P. Kofoed, Handbook of Ocean Wave Energy, Springer International Publishing, 2017.

[5] Y. Conill, "Ocean Energy Key Trends and Statistics 2022," Ocean Energy Europe, 2023.

[6] D. Cagney, "2030 Ocean Energy Vision. Industry analysis of future deployments, costs and supply chains," Ocean Energy Europe (ETIPOCEAN), 2022.

[7] I. I. R. E. A. &. O. E. Europe, "Scaling up investments in Ocean Energy Technologies," IRENA International Renewable Energy Agency & Ocean Energy Europe, 2023.

[8] J. Tan, X. Wang, A. Jarquin Laguna, H. Polinder and S. Miedema, "The Influence of Linear Permanent Magnet Generator Sizing on the Techno-Economic Performance of a Wave Energy Converter," in *13th International Symposium on Linear Drives for Industry Applications (LDIA) Linear Drives for Industry Applications (LDIA)*, Wuhan, China, 2021.

[9] C. Guo, W. Sheng, D. G. De Silva and G. Aggidis, "A Review of the Levelized Cost of Wave Energy Based on a Techno-Economic Model.," *Energies,* vol. 16, no. 5, p. 2144, 2023.

[10] G. Chang, C. A. Jones, J. D. Roberts and V. S. Neary, "A comprehensive evaluation of factors affecting the levelized cost of wave energy conversion projects," *Renewable Energy,* vol. 127, pp. 344-354, 2018.

[11] J. Tan, H. Polinder, A. Laguna, P. Wellens and S. Miedema, "The influence of sizing of wave energy converters on the techno-economic performance," *Journal of Marine Science and Engineering. ,* vol. 9, no. 1, pp. 1-25, 2021.

[12] G. Chandrasekaran, V. Sree Balaji and R. Saravanan, "Multiobjective Design Optimization of Power Take-Off (PTO) Gear Box Through NSGA II," in *Nature-Inspired Optimization in Advanced Manufacturing Processes ans Systems*, CRC Press, 2020, p. 12.

[13] J. Saveca, Y. Sun and . Z. Wang, "A Hybrid Multiobjective Optimization Based on Nondominated Sorting and Crowding Distance, with Applications to Wave Energy Converters," *International Transactions on Electrical Energy Systems,* p. 8309697, 2022.

[14] E. Amini, H. Mehdipour, E. Faraggiana, D. Golbaz, S. Mozaffari, G. Bracco and M. Neshat, "Optimization of hydraulic power take-off system settings for point absorber wave energy converter," *Renewable Energy,* vol. 194, no. 938-954, 2022.

[15] Z. He, D. Ning, Y. Gou and Z. Zhou, "Wave energy converter optimization based on differential evolution algorithm," *Energy,* vol. 246, 2022.

[16] Z. He, D. Ning, Y. Gou and R. Mayon, "Optimization of a wave energy converter square array based on the differential evolution algorithm," *Ocean Engineering,* vol. 262, 2022.

[17] S. Sirigu, L. Foglietta, G. Giorgi, M. Bonfanti, G. Cervelli, G. Bracco and G. Mattiazzo, "Techno-Economic optimisation for a wave energy converter via genetic algorithm," *Journal of Marine Science and Engineering.,* vol. 8, no. 8, 2020.

[18] M. Blanco, M. Lafoz, D. Ramírez, G. Navarro , J. Torres and L. García-Tabarés, "Dimensioning of Point Absorbers for Wave Energy Conversion by Means of Differential Evolutionary Algorithms," *IEEE Transactions on Sustainable Energy,* vol. 10, no. 3, pp. 1076-1085, 2019.

[19] M. Blanco, M. Santos-Herran, G. Navarro, J. Torres, J. Najera, M. Lafoz, I. Villalba and D. Ramírez , "Meta-heuristic optimisation approach for wave energy converter design by means of a stochastic hydrodynamic model," *IET Renewable Power Generation,* vol. 15, no. 3, pp. 548-561–561, 2021.

[20] M. Blanco, P. Moreno-Torres, M. Lafoz and D. Ramírez, "Design Parameter Analysis of Point Absorber WEC via an Evolutionary-Algorithm-Based Dimensioning Tool," *Energies,* vol. 8, no. 10, pp. 11203-11233, 2015.

[21] M. Alves, "Numerical Simulation of the Dynamics of Point Absorber Wave Energy Converters Using Frequency and Time Domain Approaches," Ph.D. dissertation, Instituto Superior Técnico- Universidad Técnica de Lisboa , Lisboa, 2012.

[22] W. Cummins, "The impulse response function and ship motions," DTIC Document, Tech. Rep., 1962.

[23] J. Wehausen, "Initial-value problem for the motion in an undulating sea of a body with fixed equilibrium position," *Journal of Engineering Mathematics,* vol. 1, pp. 1-19, 1967.

[24] Z. Yu and H. Maceda, "On the modelling of an OWC wave power system," *J. of the Kansai Society of Naval Architects,* no. 215, pp. 123-128, 1991.

[25] Z. Yu and J. Falnes, "State-space modelling of a vertical cylinder in heave," *Applied Ocean Research,* vol. 17, no. 5, pp. 265-275, 1995.

[26] J. Faiz and A. Nematsaberi, "Linear electrical generator topologies for direct-drive marine wave energy conversion- an overview," *IET RENEWABLE POWER GENERATION,* vol. 11, no. 9, pp. 1163-1176, 2017.

[27] M. Blanco, M. Vicente, J. Torres, G. Navarro, L. García-Tabarés, M. Alves and M. Lafoz, "Implementation of an energy extraction control including PTO-losses in a complete WEC model for PTO design procedure," in *13th European Wave Tidal Energy Conference (EWTEC)*, Napoles, 2019.

[28] R. Ahamed, K. McKee and I. Howard, "A Review of the Linear Generator Type of Wave Energy Converters' Power Take-Off Systems," *Sustainability,* vol. 14, p. 9936, 2022.

[29] J. Zhang, H. Yu and M. Chen, "Direct-Drive wave energy conversion with linear generator: A review of research status and challenges.," *IET Renewable Power Generation,* vol. 17, no. 4, pp. 1020-1034, 2023.

[30] A. Maria Arenas, A. J. Garrido Hernández, E. Rusu and I. Garrido Hernández, "Control Strategies Applied to Wave Energy Converters: State of the Art," *Energies,* 2020.

[31] J. Davidson, R. Genest and J. V. Ringwood, "Adaptive Control of a Wave Energy Converter.," *IEEE Transactions on Sustainable Energy,* vol. 4, no. 9, pp. 1588-1595, 2018.

[32] D. Montoya Andrade, A. De La Villa Jaén and A. García Santana, "Considering linear generator copper losses on model predictive control for a point absorber wave energy converter," *Energy Conversion and Management,* vol. 78, pp. 173-183, 2014.

[33] M. Blanco, P. Moreno-Torres, M. Lafoz and D. Ramírez, "Design Parameters Analysis of Point Absorber WEC via an evolutionary-algorithm-based Dimensioning Tool," *Energies,* vol. 8, no. 10, pp. 11203-11233, 2015.

[34] M. Blanco, M. Lafoz, D. Ramírez, G. Navarro, J. Torres and L. García-Tabares, "Dimensioning of Point Absorbers for Wave Energy Conversion by Means of Differential Evolutionary Algorithms," *IEEE Transactions on Sustainable Energy,* vol. 10, no. 3, pp. 1076-1085, 2019.

[35] E. Tedeschi and M. Molinas, "Tunable Control Strategy for Wave Energy Converters With Limited Power Takeoff Rating," *IEEE Transactions on Industrial Electronics,* vol. 59, no. 10, pp. 3838-3846, 2012.

[36] M. Blanco, M. Lafoz, A. Álvarez and M. Herreros, "Multi-objective Differential Evolutionary Algorithm for Preliminary Design of a Direct-Drive Power Take-Off," in *Proceedings of the Ninth European Wave and Tidal Energy Conference (EWTEC)*, Southampton (UK), 2011.

[37] " Surging wave energy absorption through increasing thrust and efficiency (SEA TITAN)," [Online]. Available: https://seatitan.eu/. [Accessed 2023 Marzo 1].

[38] "CORPOWER Homepage," 2019. [Online]. Available: http://www.corpowerocean.com/.

[39] "HYDROCAP ENERGY homepage," 2019. [Online]. Available: https://hydrocap.com/.

[40] "CENTIPOD homepage," 2019. [Online]. Available: http://www.ecomerittech.com/centipod.php.

[41] "WEDGE Global S.L. Homepage," 2019. [Online]. Available: http://wedgeglobal.com/.

[42] M. Blanco, M. Santos-Herrán, G. Navarro, J. Torres, J. Nájera, L. García-Tabarés and M. Lafoz, "Simplified model of a novel direct-drive PTO based on an azimuthal linear switched reluctance generator," in *14th European Wave and Tidal Energy Conference (EWTEC)*, Plymouth (UK), 2021.

[43] M. Penalba and J. V. Ringwood, "A Review of Wave-to-Wire Models for Wave Energy Converters," *Energies,* vol. 9, no. 7, p. p.506, 2016.

[44] C. Lee, "WAMIT theory manual," Massachusetts Institute of Technology (MIT), 1995.

[45] J. Falnes, Ocean Waves and Oscillating Systems, Linear Interactions Including Wave-Energy Extraction, Cambridge: Cambridge University Press, 2002.

[46] J. Grainger and W. Stevenson, Power System Analysis, New York, NY, USA; London, UK: McGraw-Hill, 1994.

[47] M. Blanco, M. Lafoz and L. García-Tabares, "Laboratory tests of linear electric machines for wave energy applications with emulation of wave energy converters and sea waves," in *Proceedings of the 2011 14th European Conference on Power Electronics and Applications*, Birmingham (UK), 2011.

[48] C. Carstensen, Eddy Currents in Windings of Switched Reluctance Machines, Aachen (Germany): PhD. Thesis. Aachen University, 2008.

[49] M. N. Sadiku and C. K. Alexander, Fundamentals of electric circuits, McGraw-Hill Higher Education, 2007.

[50] J. Torres, P. Moreno-Torres, G. Navarro, M. Blanco and M. Lafoz, "Fast Energy Storage Systems Comparison in Terms of Energy Efficiency for a Specific Application," vol. 6, pp. 40656-40672, 2018.

[51] F. García, M. Lafoz, M. Blanco and L. García-Tabares, "Efficiency Calculation of a Direct-Drive Power Take-Off," in *9th European Wave and Tidal Energy Conference (EWTEC)*, Southampton (UK), 2011.

[52] L. Hai, M. Göteman and M. Leijon, "A Methodology of Modelling a Wave Power System via an Equivalent RLC Circuit," *IEEE Transactions on Sustainable Energy,* vol. 7, no. 4, pp. 1362-1370, 2016.

[53] J. Falnes, "Wave-Energy Conversion Through Relative Motion Between Two Single-Mode Oscillating Bodies," *Journal of Offshore Mechanics and Arctic Engineering,* vol. 121, no. 1, p. 32–38, 1999.

[54] R. Genest, A. Bonnefoy, A. Clément and A. Babarit, "Effect of non-ideal power take-off on the energy absorption of a reactively controlled one degree of freedom wave energy converter," *Applied Ocean Research,* vol. 48, p. 236–243, 2014.

[55] M. Blanco, M. Vicente, J. Torres, Garc, M. Alves, M. Alves and M. Lafoz, "Implementation of an energy extraction control including PTO-losses in a complete WEC model for PTO design procedure," in *13th European Wave Tidal Energy Conference (EWTEC)*, Nápoles, 2019.

[56] K. Price and R. Storn, "Differential Evolution," Dr. Dobb's Journal, 1997. [Online]. Available: https://www.drdobbs.com/database/differential-evolution/184410166. [Accessed 3 1 2023].

[57] Z. Aimin, Q. Bo-Yang, L. Hui, Z. Shi-Zheng, S. Ponnuthurai Nagaratnam and Z. Qingfu, "Multiobjective evolutionary algorithms: A survey of the state of the art," *Swarm and Evolutionary Computation,* vol. 1, no. 1, pp. 32-49, 2011.

[58] K. Deb and N. Srinivas, “Muiltiobjective Optimization Using Nondominated Sorting in Genetic Algorithms,” *Evolutionary Computation,* vol. 2, pp. 221-248, 1994.

[59] “Aguçadora test site.,” [Online]. Available: https://www.wavec.org/en/test-sites/agucadora-test-sites.

[60] “Bilia Croo. European Marine Energy Center (EMEC),” [Online]. Available: https://www.emec.org.uk/facilities/wave-test-site/.

[61] “Orkey. European Marine Energy Center (EMEC).,” [Online]. Available: https://www.emec.org.uk/facilities/.

[62] “ Centrale Nantes offshore test site (SEMREV),” [Online]. Available: https://sem-rev.ec-nantes.fr/.

[63] “ Biscay Marine Energy Platform (BIMEP),” [Online]. Available: https://www.bimep.com/.

[64] “Plataforma Oceánica de Canarias (PLOCAN),” [Online]. Available: https://plocan.eu/.

[65] PLOCAN, “Plataforma Oceánica de Canarias,” [Online]. Available: http://www.plocan.eu/index.php/es/. [Accessed 1 3 2023].

[66] A. de Andrés, R. Guanche, J. Armesto, F. del Jesus, C. Vidal and I. Losada, “Time Domain Model for a Two-Body Heave Converter: Model and Applications.,” *Ocean Engineering,* vol. 72, pp. 116-123, 2013.

[67] K. Hasselman, “Measurements of wind-wave growth and swell decay during the Joint North Sea Wave Project (JONSWAP).,” Deutches Hydrographisches Institut , 1973.

[68] C. Cummins, “The impulse response function and ship motions,” Department of the Navy, David Taylor Model Basin, 1962.

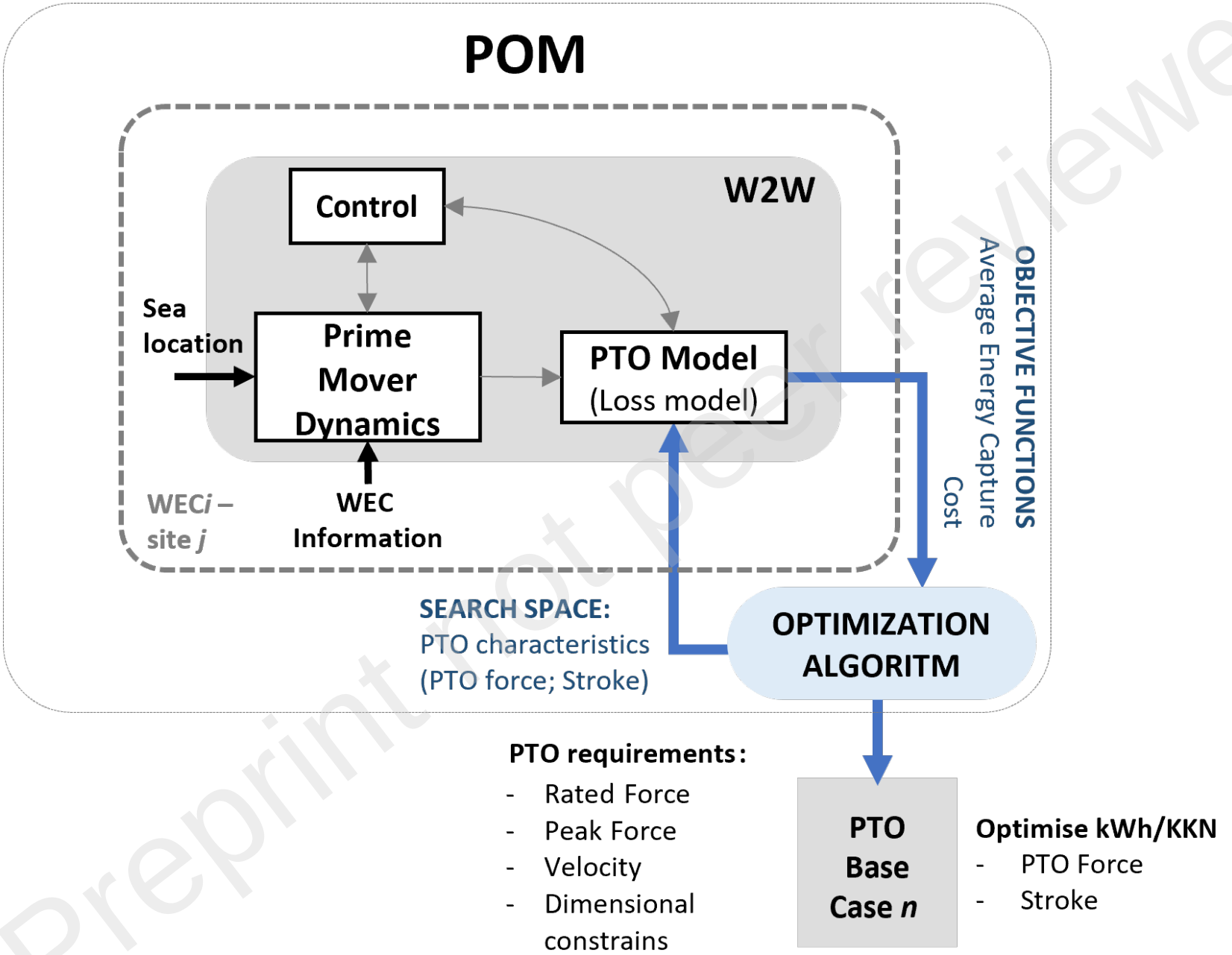

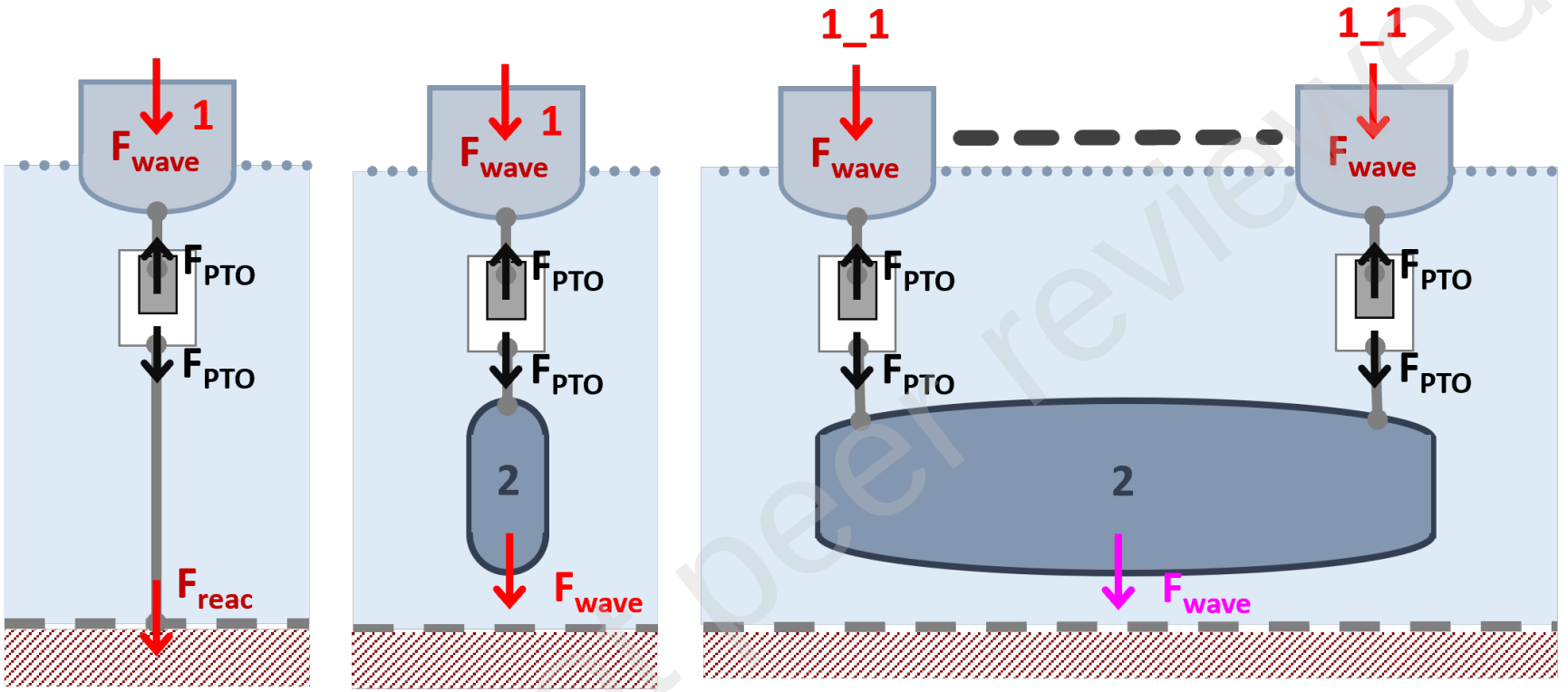

a) WEC 1-body point absorber

b) WEC 2-body point absorber

c) WEC multibody point absorber